Improved NSGA-III Algorithm and BP Fuel-cost Prediction Network for Many-objective Optimal Power Flow Problems

Jie Qian, Hongyu Long*, Yi Long, and Chenxu Zhao

***Abstract*—To effectively handle the many-objective optimal power flow (MOOPF) problems considering the simultaneous reduction of power loss, emission and fuel cost, an improved NSGA-III (INSGA-III) algorithm is put forward in this paper. In detail, the proposed INSGA-III algorithm adopts the competitive solutions preliminarily optimized by traditional NSGA-III method as the initial population and integrates the novel adaptive dominant (NAD) strategy. Comparing with the original NSGA-III algorithm, INSGA-III obtains the more preferable Pareto front (PF) with uniform distribution. More significantly, an entirely new BP fuel-cost prediction network is proposed to explore the potential elite power flow (EPL) solutions. These EPL solutions determined around the best compromise solution (BCS) of INSGA-III algorithm provide decision-makers with more and better scheduling schemes. The effectiveness and superiorities of proposed INSGA-III algorithm and BP fuel-cost prediction model are verified by both dual-objective and triple-objective MOOPF simulation experiments. In general, this paper presents an innovative way to solve the complex engineering problems by computer technologies represented by intelligent algorithms and neural networks.**

***Index Terms*—Improved NSGA-III algorithm, Many-objective optimal power flow, Adaptive dominant strategy, BP fuel-cost prediction network, Computer technologies**

I. Introduction

IN order to realize the economic and safe operation of power systems, the high-quality dispatching schemes which can reduce the fuel cost, active power loss and emission are needed. At present, the optimal power flow (OPF) problems considering only single objective cannot satisfy the various needs of users. Therefore, more scholars focus on the many-objective OPF (MOOPF) problems which aim to achieve the simultaneous reduction of two or three goals [1-4].

To solve MOOPF problems is actually to seek a feasible Pareto optimal set (POS) which meets all system constraints. According to the commonly-used fuzzy affiliation function, the best compromise solution (BCS) of MOOPF problem can be determined from obtained POS set [5]. Then, adjusting the control variables based on the BCS of MOOPF problem can realize the desired operating state of power grids.

The non-convexity and high-dimensional characteristics make traditional methods unsuitable for MOOPF problems. While intelligent algorithms provide the effective way to solve this complex optimization problem. Now, the strength Pareto evolutionary algorithm [6], the cuckoo search algorithm [7], the novel hybrid bat algorithm [8] and the artificial fish swarm algorithm [2] published recently are all appropriate for solving MOOPF problems.

A. Contributions

Two main contributions, the improved NSGA-III (INSGA-III) algorithm and an effective BP fuel-cost prediction network, are put forward and applied to MOOPF problems.

1) INSGA-III Algorithm

In this paper, the NSGA-III algorithm, which is often regarded as one evaluation benchmark for multi-objective algorithms, is adopted to handle MOOPF problems. Since the relatively-scattered distribution of Pareto front (PF) obtained by the standard NSGA-III algorithm, the modified INSGA-III algorithm is put forward. The initial population of suggested INSGA-III algorithm is preliminarily screened by NSGA-II algorithm and the novel adaptive dominant (NAD) strategy is integrated into INSGA-III algorithm as well.

To validate the applicability of INSGA-III algorithm, two dual-objective and one triple-objective MOOPF experiments are conducted on the IEEE 30-node system. The generational distance (GD) and hyper-volume (HV) indexes quantitatively demonstrate that compared with the original NSGA-III algorithm, INSGA-III method has obvious advantages in PF-uniformity and PF-diversity. In addition, the suggested INSGA-III algorithm also achieves the higher-quality BCS solutions, which is conducive to the optimized operating status of power systems.

2) BP Fuel-cost Prediction Network

Furthermore, a fire new fuel-cost predicting model based on BP network is proposed to search the possible elite power-flow (EPL) solutions. Explored in a small range close to the current BCS, EPL solutions realize zero constraints violation and dominate the final BCS solution of INSGA-III method. Three experiments with different goal combinations

Manuscript received October 31, 2020; revised February 6, 2021.

Jie Qian is a PhD candidate of the School of Computer Science and Technology, Chongqing University of Posts and Telecommunications, Chongqing 400065, China. (e-mail: qianjie@126.com).

Hongyu Long is a senior engineer of Key Laboratory of Complex Systems and Bionic Control, Chongqing University of Posts and Telecommunications, Chongqing 400065, China (corresponding author, Tel: 13996108500; e-mail: longhongyu20@163.com).

Yi Long is a senior engineer of State Grid Chongqing Electric Power Company Marketing Service Center, Chongqing 401123, China (e-mail: 156376604 @qq.com).

Chenxu Zhao is a senior engineer of Inner Mongolia Power (Group) Co., Ltd, Inner Mongolia Power Economy and Technology Research Institute, Hohhot 010010, China (e-mail: 248349577@qq.com).

prove that the presented BP fuel-cost prediction network is not only suitable for dual-objective MOOPF simulation problems, but also for the more complex triple-objective ones.

B. Structure

The structure of this paper is set as follows. Three goals and two kinds of constraints for MOOPF problems are given in Section II. Section III introduces two major contributions of this paper including INSGA-III algorithm and BP fuel-cost prediction model. Then, detailed results of three MOOPF cases to verify the superiority of INSGA-III algorithm and fuel-cost prediction model are given in Section IV. In the final, Section V gives the conclusion of this paper.

II. MOOPF MODEL

The mathematical model of MOOPF studied in this paper is mainly composed of three objective functions and system constraints.

A. Goals

The fuel cost (F_{cost}), power loss (F_{loss}) and emission (F_{emis}) are optimized by INSGA-III algorithm. The formulas of mentioned goals are shown as (1) ~ (3) [7, 9, 10].

$$F_{\cos t}(\$/h)=\sum_{i=1}^{N_G}(a_i+b_iP_{Gi}+c_iP_{Gi}^2) \tag{1}$$

$$F_{loss}(MW)=\sum_{k=1}^{N_L}c_k[V_i^2+V_j^2-2V_iV_j\cos(\delta_i-\delta_j)] \tag{2}$$

$$F_{emis}(ton/h)=\sum_{i=1}^{N_G}[\alpha_iP_{Gi}^2+\beta_iP_{Gi}+\gamma_i+\eta_i\exp(\lambda_iP_{Gi})] \tag{3}$$

where N_G, N_L are the numbers of generators and transmission lines. V_i and δ_i are the voltage-magnitude and voltage-angle of ith node. The other special symbols are clarified in literatures [5, 11, 12].

B. Constraints

The MOOPF problems are restricted by equality constraints and inequality ones.

1) Equality Constraints

Two equality constraints, the power balance equations in essence, are shown as (4) and (5) [13-15].

$$P_{Gi}-P_{Di}-V_i\sum_{j\in N_i}V_j(G_{ij}\cos\delta_{ij}+B_{ij}\sin\delta_{ij})=0, i\in N \tag{4}$$

$$\begin{gathered}Q_{Gi}-Q_{Di}-V_i\sum_{j\in N_i}V_j(G_{ij}\sin\delta_{ij}-B_{ij}\cos\delta_{ij})=0\\ i\in N_{PQ}\ \ \delta_{ij}=\delta_i-\delta_j\end{gathered} \tag{5}$$

2) Inequality Constraints on Control Variables

The inequality restrictions on the generator node voltage (V_G), the generator active power output at PV node (P_G), the tap ratios of transformer (T) and the reactive power injection (Q_C) are shown as (6) ~ (9) [5, 16].

$$V_{Gi}^{\min}\le V_{Gi}\le V_{Gi}^{\max},\ i\in N_G \tag{6}$$

$$P_{Gi}^{\min}\le P_{Gi}\le P_{Gi}^{\max}, i\in N_G (i\ne 1) \tag{7}$$

$$T_i^{\min}\le T_i\le T_i^{\max},\ i\in N_T \tag{8}$$

$$Q_{Ci}^{\min}\le Q_{Ci}\le Q_{Ci}^{\max},\ i\in N_C \tag{9}$$

3) Inequality Constraints on State Variables

The inequality restrictions on the generator active power at slack node (P_{G1}), the load node voltage (V_L), the generator reactive power (Q_G) and the apparent power of transmission line (S) are shown as (10) ~ (13) [1, 17].

$$P_{G1}^{\min}\le P_{G1}\le P_{G1}^{\max} \tag{10}$$

$$V_{Li}^{\min}\le V_{Li}\le V_{Li}^{\max},\ i\in N_{PQ} \tag{11}$$

$$Q_{Gi}^{\min}\le Q_{Gi}\le Q_{Gi}^{\max},\ i\in N_G \tag{12}$$

$$S_i^{\max}-S_i\ge 0,\ i\in N_L \tag{13}$$

where N_T, N_C, N_{PQ} are the numbers of transformers, compensators and PQ nodes. The other special symbols are clarified in literatures [5, 18, 19].

C. Constraints Processing

As the termination condition of Newton-Raphson power flow calculation, two equality constraints do not need the additional treatment. Therefore, this paper focuses on the processing of two kinds of inequality constraints.

1) Treatment of Unqualified Control Variables

The unqualified control variables which violate (6) ~ (9) are regulated according to (14).

$$Con_i=\begin{cases}Con_i^{\max} & if\ \ Con_i>Con_i^{\max}\\ Con_i^{\min} & if\ \ Con_i<Con_i^{\min}\end{cases} \tag{14}$$

where Con_i^{max} indicates the maximum value of the ith control variables set and the Con_i^{min} is the minimal one.

2) Treatment of Unqualified State Variables

The unqualified state variables which violate (10) ~ (13) will be filtered out based on the constraints-violation and objective-function values. The adoption priorities, also called the *Rank* index, of candidate power-flow schemes are determined according to (15) and (16). The acquisition of *Rank* is inspired by the non-inferior sorting idea proposed by Deb [20-22]. In detail, the ith power-flow solution will be given a higher adoption priority when condition (15) or (16) is met.

$$Cvio(S(Con_i))<Cvio(S(Con_j)) \tag{15}$$

$$\begin{cases}Cvio(S(Con_i))=Cvio(S(Con_j))\\ Ob_m(S(Con_i))\le Ob_m(S(Con_j)),\forall m\in\{1,2,...,N_o\}\\ Ob_n(S(Con_i))<Ob_n(S(Con_j)),\exists n\in\{1,2,...,N_o\}\end{cases} \tag{16}$$

where $Cvio(S(Con_i))$ defined as (17) is the constraints violation of the ith power-flow scheme. $Ob_m(S(Con_i))$ is the mth objective value of the ith power-flow scheme. Besides, N_o is the number of goals optimized simultaneously.

$$\begin{aligned}Cvio(S(Con_i))=&|Cvio_{\_P}(S(Con_i))|+|Cvio_{\_V}(S(Con_i))|\\&+|Cvio_{\_Q}(S(Con_i))|+|Cvio_{\_S}(S(Con_i))|\end{aligned} \tag{17}$$

where $Cvio_{\_P}(S(Con_i))$, $Cvio_{\_V}(S(Con_i))$, $Cvio_{\_Q}(S(Con_i))$ and $Cvio_{\_S}(S(Con_i))$ are the constraints violations of ith scheme which respectively violate (10) ~ (13).

III. ALGORITHM AND PREDICTION MODEL

The novel INSGA-III algorithm and BP fuel-cost prediction network, which are put forward to explore the satisfactory power flow scheduling schemes, are introduced as follows.

A. Modified INSGA-Ⅲ Algorithm

The application of basic NSGA-III algorithm on MOOPF problems can refer to [5, 8, 23]. Aiming at the deficiencies of NSGA-III, two major measures are integrated into INSGA-III algorithm which greatly improve the performance for solving MOOPF problems.

1) Optimization of Initial Population

Due to the poor PF-distribution obtained by original NSGA-III method, an innovative idea of conducting the preliminary screening for initial population is put forward. In this paper, the typical NSGA-II algorithm is adopted to optimize the initial population of presented INSGA-III algorithm. The POS_{ns2} set obtained by NSGA-II method after Ite_{ns2}(max) iterations is taken as the input of INSGA-III algorithm, which is helpful to make basic adjustments of PF-distribution at the initial stage.

2) NAD Dominant Strategy

In order to avoid the loss of high-quality power flow schemes, the proposed NAD dominant strategy is adopted in the iterative process of INSGA-III algorithm. The NAD strategy can be described as (18).

$$S_{k+1}^{valid}(Con_i)=\begin{cases} S_k^{valid}(Con_i), \\ if\ S_k^{valid}(Con_i)\ do\min ates\ \ S_{k+1}^{INSGA3}(Con_i) \\ S_{k+1}^{INSGA3}(Con_i), \\ if\ S_{k+1}^{INSGA3}(Con_i)\ do\min ates\ S_k^{valid}(Con_i) \end{cases} \tag{18}$$

where S_{k+1}^{INSGA3} (Con_i) is the ith power flow solution updated based on INSGA-III model at the (k+1)th iteration. S_{k+1}^{valid} (Con_i) indicates the final ith power flow solution of INSGA-III algorithm after the (k+1)th iteration.

In other word, the $S_k^{valid}(Con_i)$ will remain unchanged at the (k+1)th iteration when S_{k+1}^{INSGA3} (Con_i) is not superior to S_k^{valid} (Con_i). The dominant relationship of different schemes can be judged according to (15) and (16). The effective NAD strategy can reserve the elite power flow solutions to the great extent.

The main flow-chart of presented INSGA-III algorithm on MOOPF problems is summarized as Fig. 1. The $Ite_{ns3}(max)$ and POS_{ns3} indicate the maximum iteration and the final POS set of INSGA-III method. Additionally, the models of standard NSGA-II and NSGA-III algorithms can refer to [5, 20, 21].

B. BP Fuel-cost Prediction Model

In this paper, a novel BP fuel-cost prediction model, which is applicable for double-objective and triple-objective MOOPF problems, is proposed. Taking the basic fuel cost as the entry point, the proposed BP prediction model is able to search the EPL solutions near the current BCS solution of INSGA-III. The applications of neural network can refer to [24, 25].

The main steps of suggested fuel-cost prediction network are shown in TABLE I. In TABLE I, three indicators including the mean absolute error (MAE), the mean absolute percentage error (MAPE) and the root mean squared error (RMSE) are adopted to evaluate the performance of different predictive models. Three mentioned indexes are defined as (19) ~ (21) [26].

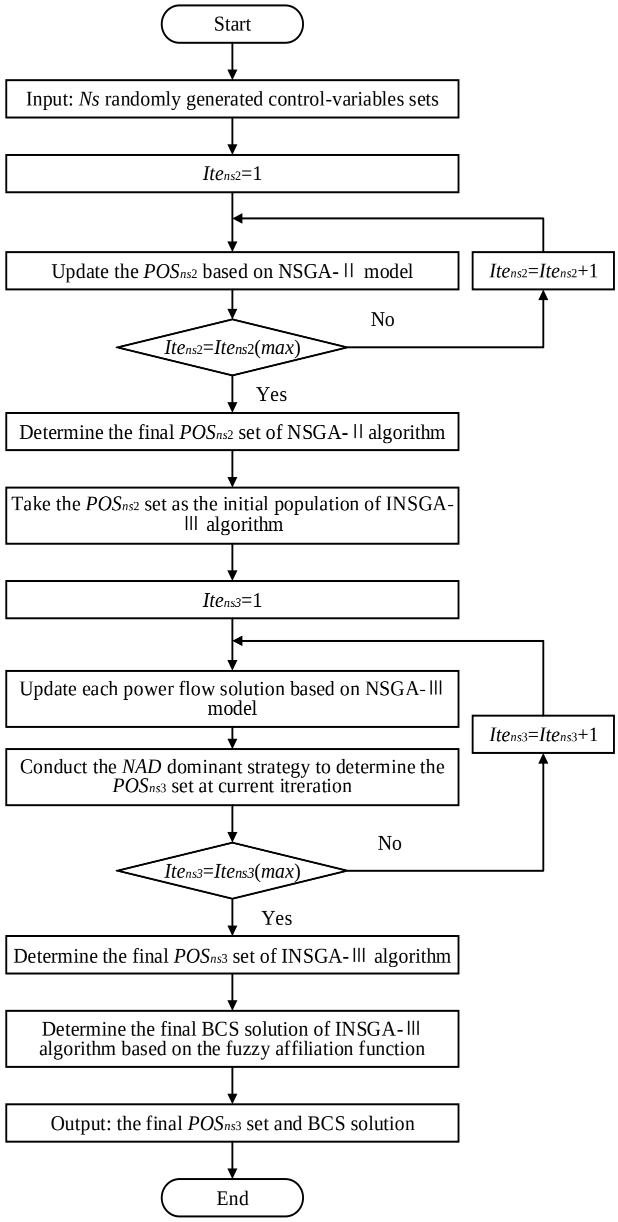

Fig. 1. Flow-chart of INSGA-III algorithm

$$MAE=\frac{1}{Ns}\sum_{i=1}^{Ns}\left|Fuel_{real}(i)-Fuel_{pre}(i)\right| \tag{19}$$

$$MAPE=\frac{1}{Ns}\sum_{i=1}^{Ns}\left|\frac{Fuel_{real}(i)-Fuel_{pre}(i)}{Fuel_{real}(i)}\right|\times 100\% \tag{20}$$

$$RMSE=\sqrt{\frac{\sum_{i=1}^{Ns}(Fuel_{real}(i)-Fuel_{pre}(i))^2}{Ns}} \tag{21}$$

where Ns is the population size of INSGA-III algorithm and $Fuel_{real}$ is the real fuel cost calculated by Newton-Raphson power flow method.

IV. Experiments and Results

Three MOOPF cases on IEEE 30-node system with different goal combinations shown in TABLE II are studied. The structure of standard 30-node system is shown in Fig. 2 and the effective operating ranges of electrical equipment are clarified in [5, 27, 28].

TABLE I
MAIN STEPS OF BP FUEL-COST PREDICTION NETWORK

Begin
Input 2000 power flow scheduling schemes and the corresponding F_{cost} values;
for *i*=1:5
Select the random 1900 schemes for network-training ($Input_{train}$) and the other 100 schemes for testing ($Input_{test}$);
Identify the 1900 training-output ($Output_{train}$) and 100 testing-output ($Output_{test}$);
Perform the data normalization;
% Clarify the structure of BP network
$N_{BP(i)}$=newff ($Input_{train}$, $Output_{train}$,[24,24]);
$N_{BP(i)}$.trainParam.epochs=30;
$N_{BP(i)}$.trainParam.lr=0.1;
$N_{BP(i)}$.trainParam.goal=0.000001;
Generate the *i*th candidate fuel-cost prediction network $N_{BP(i)}$;
Predict the fuel cost of $Input_{test}$ set ($OutBP_{test}$) according to $N_{BP(i)}$ model;
Perform the inverse-normalization on $OutBP_{test}$ set to obtain the predictive fuel cost value ($Fuel_{pre}$);
Save the *i*th BP model $N_{BP(i)}$;
end for
Evaluate the quality of five BP fuel-cost models based on $Output_{test}$ and $Fuel_{pre}$ values;
Determine the relatively-best model N_{BP}^{best};
Sch_{all}=50;
Sch_{elite}=10;
Input the control variables set of BCS solution obtained by INSGA-III algorithm (C_{BCS}^{NSGA});
Set the valid ranges of BP exploration within [0.999C_{BCS}^{NSGA}, 1.001C_{BCS}^{NSGA}];
Randomly generate Sch_{all} control-variables sets within the valid ranges;
Regulate the unqualified Sch_{all} sets based on (14);
Obtain the $Fuel_{pre}$ values of Sch_{all} sets based on N_{BP}^{best} network;
Pick out the Sch_{elite} elite schemes with smaller $Fuel_{pre}$ values from Sch_{all} candidate schemes;
Perform the Newton-Raphson power flow calculation to Sch_{elite} schemes and obtain the real F_{cost}, F_{emis} and F_{loss} values;
Determine the EPL solutions which dominate the current BCS from Sch_{elite} schemes;
End

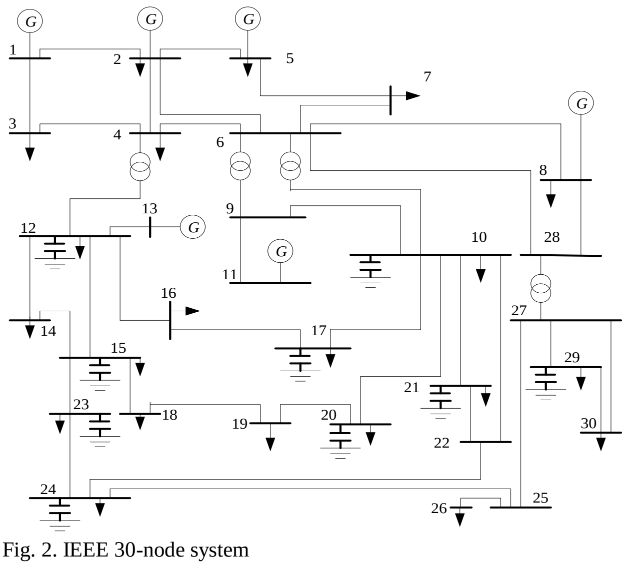

Fig. 2. IEEE 30-node system

A. Parameters

The influence of $Ite_{ns2}(max)$ and $Ite_{ns3}(max)$, two involved maximum iterations of INSGA-III algorithm, in solving MOOPF problems is firstly discussed.

Fig. 3 gives the PFs of CASE-1 with different maximum iterations. It clearly indicates that the $Ite_{ns3}(max)$=150 ($Ite_{ns2}(max)$=50) only finds the feasible PF while $Ite_{ns3}(max)$ =150 ($Ite_{ns2}(max)$=70) achieves the relatively-optimal PF. In addition, Fig. 4 which gives the PFs of CASE-2 with different iterations also demonstrates INSGA-III algorithm can find the superior PF with $Ite_{ns3}(max)$=150 ($Ite_{ns2}(max)$=70). Therefore, it is reasonable to set the $Ite_{ns2}(max)$, $Ite_{ns3}(max)$ to 70 and 150, respectively.

The parameters of NSGA-II, which is used for the preliminary optimization of INSGA-III algorithm, can refer to [5]. Furthermore, the other parameters of proposed INSGA-III algorithm and the basic NSGA-III algorithm for comparison are set as TABLE III.

B. Verification Experiments

Massive results of three MOOPF cases are used to verify the applicability of INSGA-III method and BP prediction model.

1) CASE-1

The PFs of bi-objective CASE-1 obtained by traditional NSGA-III and modified INSGA-III algorithms are, respectively, given in Fig. 5 and Fig. 6. Intuitively, the PF-distribution of INSGA-III algorithm is much better than the one of NSGA-III method.

Besides, the BCS and comparison results of CASE-1 are given in TABLE IV. TABLE IV shows that comparing with NSGA-III method, INSGA-III algorithm achieves the obviously smaller F_{cost} value with small differences in F_{emis} goal. Furthermore, the BCS solution of INSGA-III method including 0.2369 ton/h of F_{emis} and 831.6315 \$/h of F_{cost} dominates the ones of published MODFA and NHBA methods.

TABLE II
CASE-SETTING

Goal	CASE-1	CASE-2	CASE-3
F_{cost}	√	√	√
F_{emis}	√		√
F_{loss}		√	√
Repeated number	30	30	30

TABLE III
ALGORITHM PARAMETERS

Algorithm	NSGA-III	INSGA-III
Ns	100	100
$Ite_{ns2}(max)$	-	70
$Ite_{ns3}(max)$	300	150
mutation indictor/ percentage	20/1	20/1
crossover indictor/ percentage	20/0.1	20/0.1
number of divisions	10	10

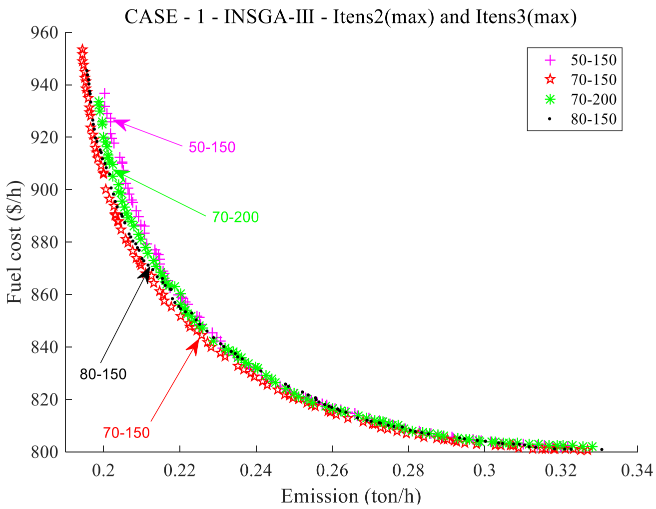

Fig. 3. PF of CASE-1 with different iterations

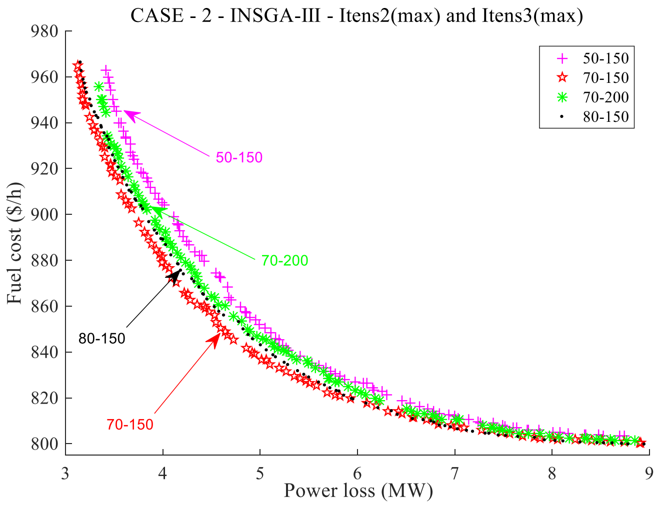

Fig. 4. PF of CASE-2 with different iterations

Meanwhile, TABLE V gives the minimal F_{cost} and minimal F_{emis} of CASE-1. It indicates that the proposed INSGA-III algorithm finds 800.8147 \$/h of minimal F_{cost} and 0.1944 ton/h of minimal F_{emis}. In general, two minimal goals found by INSGA-III algorithm in CASE-1 are both superior to basic NSGA-III algorithm.

To quantitatively evaluate the PF-distribution and PF-diversity, the GD and HV indicators are adopted in this paper. The application of GD and HV indexes on MOOPF problems can refer to [5, 29]. In detail, the boxplots, the average and deviation of two related indictors for CASE-1 are given in Fig. 7 and TABLE VI. The smaller GD-average value shows the uniform-distribution of PF obtained by INSGA-III and the larger HV-average shows the better diversity. Then, the closer boxplot, the smaller GD and HV deviations prove the operational stability of INSGA-III algorithm.

More notably, five candidate BP predictive models which take the basic fuel cost as the entry-point are built for CASE-1. TABLE VII, which gives the MAE, MAPE, RMSE errors of five candidate models, indicates that the $N_{BP(5)}$ with three smaller errors achieves the relatively-best performance. Fig. 8 and Fig. 9, respectively, show the fitting results and relative error of CASE-1 based on $N_{BP(5)}$ network. It turns out the proposed BP fuel-cost model can effectively predict F_{cost} value based on the 24-dimensional control variables.

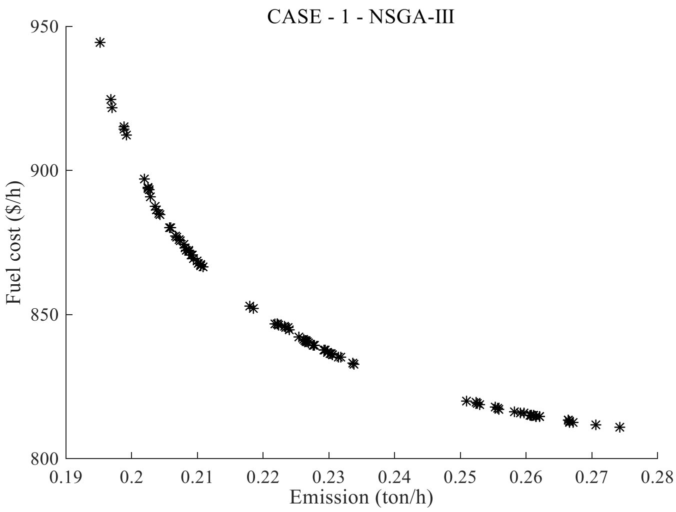

Fig. 5. PF of CASE-1 obtained by NSGA-III

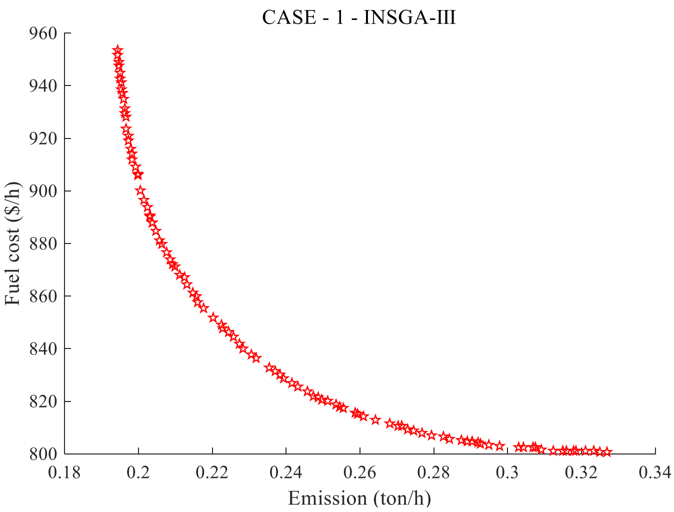

Fig. 6. PF of CASE-1 obtained by INSGA-III

TABLE IV
BCS AND COMPARISON OF CASE-1

Variables	CASE-1			
	NSGA-III	INSGA-III	MODFA [5]	NHBA [8]
P_{G2}(MW)	59.0446	60.3662	56.6689	58.1990
P_{G5}(MW)	27.8098	25.5531	28.2520	25.6741
P_{G8}(MW)	34.9985	35.0000	35.0000	27.0218
P_{G11}(MW)	27.3828	26.1379	26.3123	26.3626
P_{G13}(MW)	28.1427	23.8845	25.7403	31.3704
V_{G1}(p.u.)	1.0588	1.0411	1.0989	1.1000
V_{G2}(p.u.)	1.0457	1.0270	1.0909	1.0890
V_{G5}(p.u.)	1.0240	0.9873	1.0676	1.0537
V_{G8}(p.u.)	1.0269	0.9893	1.0804	1.0639
V_{G11}(p.u.)	1.0683	1.0571	1.0966	1.0880
V_{G13}(p.u.)	1.0861	1.0508	1.0999	1.0517
T_{11}(p.u.)	0.9999	0.9928	1.0151	1.0711
T_{12}(p.u.)	0.9007	0.9732	0.9493	0.9304
T_{15}(p.u.)	0.9759	0.9618	0.9903	1.1000
T_{36}(p.u.)	0.9370	0.9387	0.9666	1.0097
Q_{C10}(p.u.)	0.0022	0.0300	0.0000	0.0299
Q_{C12}(p.u.)	0.0341	0.0303	0.0423	0.0473
Q_{C15}(p.u.)	0.0000	0.0198	0.0463	0.0157
Q_{C17}(p.u.)	0.0045	0.0124	0.0462	0.0450
Q_{C20}(p.u.)	0.0201	0.0176	0.0243	0.0291
Q_{C21}(p.u.)	0.0302	0.0500	0.0421	0.0333
Q_{C23}(p.u.)	0.0478	0.0396	0.0415	0.0500
Q_{C24}(p.u.)	0.0454	0.0263	0.0198	0.0235
Q_{C29}(p.u.)	0.0477	0.0160	0.0198	0.0088
F_{emis} (ton/h)	0.2278	**0.2369**	0.2432	0.2375
F_{cost}($/h)	839.1713	**831.6315**	831.6652	832.6471

TABLE V
MINIMAL SOLUTIONS OF CASE-1

Variables	CASE-1			
	Minimal F_{cost}		Minimal F_{emis}	
	NSGA-III	INSGA-III	NSGA-III	INSGA-III
P_{G2}(MW)	50.9118	49.7022	72.6508	72.1929
P_{G5}(MW)	22.3327	21.4528	47.7526	50.0000
P_{G8}(MW)	32.5199	20.2328	34.9127	34.8866
P_{G11}(MW)	15.8096	13.0020	29.9436	30.0000
P_{G13}(MW)	22.5486	12.0609	40.0000	39.9993
V_{G1}(p.u.)	1.0628	1.0830	1.0566	1.0249
V_{G2}(p.u.)	1.0517	1.0630	1.0447	1.0157
V_{G5}(p.u.)	1.0152	1.0294	0.9907	0.9842
V_{G8}(p.u.)	1.0241	1.0352	1.0365	0.9840
V_{G11}(p.u.)	1.0251	1.0340	1.0400	1.0397
V_{G13}(p.u.)	1.0781	1.0677	1.0605	1.0119
T_{11}(p.u.)	0.9954	1.0147	0.9770	1.0104
T_{12}(p.u.)	0.9255	0.9343	0.9180	0.9781
T_{15}(p.u.)	1.0035	1.0757	1.0517	0.9485
T_{36}(p.u.)	0.9304	1.0080	0.9295	0.9518
Q_{C10}(p.u.)	0.0000	0.0306	0.0059	0.0339
Q_{C12}(p.u.)	0.0442	0.0216	0.0421	0.0361
Q_{C15}(p.u.)	0.0051	0.0414	0.0149	0.0268
Q_{C17}(p.u.)	0.0052	0.0369	0.0159	0.0071
Q_{C20}(p.u.)	0.0150	0.0281	0.0131	0.0158
Q_{C21}(p.u.)	0.0286	0.0233	0.0384	0.0467
Q_{C23}(p.u.)	0.0396	0.0199	0.0364	0.0472
Q_{C24}(p.u.)	0.0446	0.0269	0.0402	0.0282
Q_{C29}(p.u.)	0.0482	0.0488	0.0402	0.0353
F_{emis} (ton/h)	0.2743	0.3268	0.1952	**0.1944**
F_{cost}($/h)	810.7470	**800.8147**	944.2417	953.3882

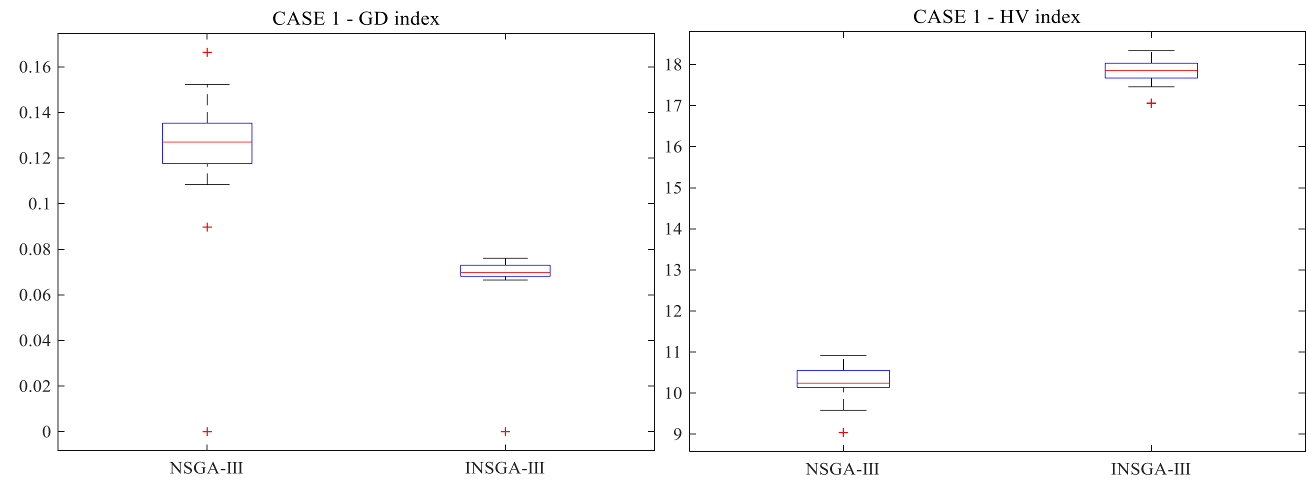

Fig. 7. Boxplot of GD and HV indexes for CASE-1

TABLE VI
GD AND HV OF CASE-1

Quantitative indicators		GD		HV	
		Average	Deviation	Average	Deviation
CASE-1	NSGA-III	0.1241	0.0280	10.2723	0.3843
	INSGA-III	0.0682	0.0132	17.8356	0.2914

TABLE VII
ERRORS OF CANDIDATE NETWORKS FOR CASE-1

Networks	MAE	MAPE	RMSE
$N_{BP(1)}$	0.0455	5.4167E-05	0.0836
$N_{BP(2)}$	0.0593	7.0785E-05	0.0916
$N_{BP(3)}$	0.0610	7.2672E-05	0.0971
$N_{BP(4)}$	0.0599	7.1354E-05	0.1086
$\mathbf{N_{BP(5)}}$	**0.0441**	**5.2533E-05**	**0.0781**

TABLE VIII
Sch_{elite} CANDIDATE ELITE SOLUTIONS OF CASE-1

Candidate	***Solution$_1$***	*Solution$_2$*	*Solution$_3$*	***Solution$_4$***	*Solution$_5$*
$Fuel_{pre}$	**832.4020**	832.4279	832.4353	**832.4366**	832.4415
F_{cost}	**831.5722**	831.5168	831.6050	**831.6046**	831.6054
F_{emis}	**0.2369**	0.2370	0.2370	**0.2369**	0.2370
Dominance	√	-	-	√	-
Candidate	***Solution$_6$***	*Solution$_7$*	*Solution$_8$*	***Solution$_9$***	***Solution$_{10}$***
$Fuel_{pre}$	**832.4435**	832.4438	832.4497	**832.4513**	**832.4516**
F_{cost}	**831.6101**	831.5956	831.5835	**831.5910**	**831.5606**
F_{emis}	**0.2369**	0.2370	0.2370	**0.2369**	**0.2369**
Dominance	√	-	-	√	√

Then, TABLE VIII gives the Sch_{elite} candidate elite solutions of CASE-1. It includes the predictive and real fuel cost, the real emission and the dominant relationship compared with the BCS of INSGA-III. It turns out five EPL solutions are determined by $N_{BP(5)}$ network.

In the end, five EPL solutions of CASE-1 which dominates the current BCS are given in TABLE IX. By adjusting the electrical devices based on the control variables of obtained EPL solutions, the more desirable grid operation state can be realized.

2) CASE-2

The PFs of another bi-objective CASE-2 obtained by NSGA-III and novel INSGA-III algorithms are given in Fig. 10 and Fig. 11, respectively. Fig. 11 shows comparing with NSGA-III, the suggested INSGA-III algorithm achieves the PF with better distribution-uniformity.

For CASE-2, the BCS solutions determined by NSGA-III, INSGA-III methods and the ones found by published NHBA, HFBA-COFS algorithms are given in TABLE X. It indicates the BCS of INSGA-III method including 832.0140 \$/h of F_{cost} and 5.0766 MW of F_{loss} is more advantageous than the ones of NSGA-III and HFBA-COFS methods. For INSGA-III and NHBA algorithms, although the F_{loss} values obtained are similar, the former finds the significantly-smaller F_{cost} value.

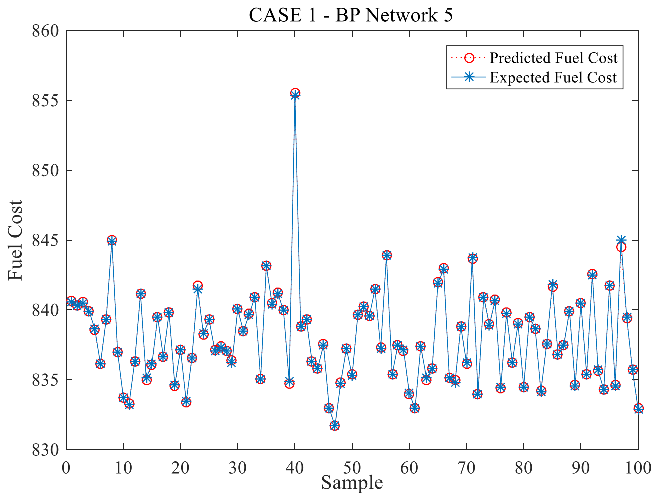

Fig. 8. Fitting results of CASE-1

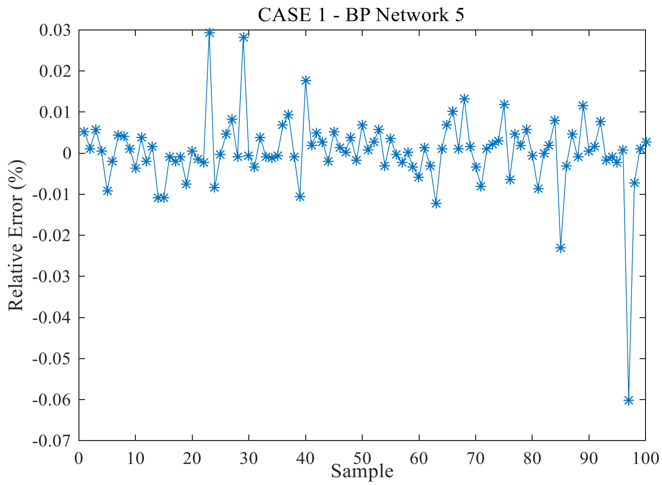

Fig. 9. Relative error of CASE-1

TABLE IX
EPL SOLUTIONS OF CASE-1

Variables	CASE-1				
	EPL_1	EPL_2	EPL_3	EPL_4	EPL_5
P_{G2}(MW)	60.3738	60.3412	60.3425	60.3597	60.3235
P_{G5}(MW)	25.5367	25.5499	25.5757	25.5520	25.5764
P_{G8}(MW)	35.0000	35.0000	35.0000	34.9689	34.9788
P_{G11}(MW)	26.1245	26.1611	26.1309	26.1326	26.1237
P_{G13}(MW)	23.8720	23.8804	23.8662	23.9077	23.9031
V_{G1}(p.u.)	1.0407	1.0403	1.0406	1.04069	1.0415
V_{G2}(p.u.)	1.0277	1.0273	1.0276	1.0269	1.0269
V_{G5}(p.u.)	0.9879	0.9880	0.9878	0.9882	0.9882
V_{G8}(p.u.)	0.9898	0.9897	0.9893	0.9896	0.9900
V_{G11}(p.u.)	1.0579	1.0577	1.0569	1.0577	1.0577
V_{G13}(p.u.)	1.0517	1.0517	1.0513	1.0510	1.0501
T_{11}(p.u.)	0.9929	0.9927	0.9927	0.9928	0.9929
T_{12}(p.u.)	0.9732	0.9732	0.9732	0.9732	0.9733
T_{15}(p.u.)	0.9618	0.9618	0.9618	0.9618	0.9618
T_{36}(p.u.)	0.9387	0.9387	0.9387	0.9387	0.9387
Q_{C10}(p.u.)	0.0300	0.0300	0.0300	0.0300	0.0300
Q_{C12}(p.u.)	0.0303	0.0303	0.0303	0.0303	0.0303
Q_{C15}(p.u.)	0.0198	0.0198	0.0198	0.0198	0.0198
Q_{C17}(p.u.)	0.0124	0.0124	0.0124	0.0124	0.0124
Q_{C20}(p.u.)	0.0176	0.0176	0.0176	0.0176	0.0176
Q_{C21}(p.u.)	0.0500	0.0500	0.0500	0.0500	0.0500
Q_{C23}(p.u.)	0.0396	0.0396	0.0396	0.0396	0.0396
Q_{C24}(p.u.)	0.0263	0.0263	0.0263	0.0263	0.0263
Q_{C29}(p.u.)	0.0160	0.0160	0.0160	0.0160	0.0160
F_{cost} (\$/h)	831.5722	831.6046	831.6101	831.5910	831.5606
F_{emis} (ton/h)	0.2369	0.2369	0.2369	0.2369	0.2369

TABLE X
BCS AND COMPARISON OF CASE-2

Variables	CASE-2			
	NSGA-III	INSGA-III	NHBA [8]	HFBA-COFS [29]
P_{G2}(MW)	53.7299	52.2117	54.7737	53.1358
P_{G5}(MW)	32.9401	30.0472	34.1273	32.4210
P_{G8}(MW)	34.9692	35.0000	35.0000	35.0000
P_{G11}(MW)	27.7402	29.8958	26.3571	26.5747
P_{G13}(MW)	23.7350	22.2722	20.5383	22.2063
V_{G1}(p.u.)	1.0851	1.1000	1.0993	1.1000
V_{G2}(p.u.)	1.0684	1.0874	1.0857	1.0881
V_{G5}(p.u.)	1.0432	1.0645	1.0629	1.0718
V_{G8}(p.u.)	1.0546	1.0729	1.0749	1.0767
V_{G11}(p.u.)	1.0941	1.1000	1.0754	1.0938
V_{G13}(p.u.)	1.0926	1.1000	1.0984	1.0951
T_{11}(p.u.)	0.9441	1.0285	0.9911	1.0304
T_{12}(p.u.)	1.0115	0.9098	0.9871	0.9469
T_{15}(p.u.)	0.9852	0.9803	0.9802	1.0078
T_{36}(p.u.)	0.9409	0.9709	0.9628	0.9818
Q_{C10}(p.u.)	0.0384	0.0082	0.0169	0.0489
Q_{C12}(p.u.)	0.0146	0.0500	0.0000	0.0314
Q_{C15}(p.u.)	0.0475	0.0203	0.0297	0.0324
Q_{C17}(p.u.)	0.0121	0.0362	0.0391	0.0460
Q_{C20}(p.u.)	0.0147	0.0462	0.0108	0.0265
Q_{C21}(p.u.)	0.0434	0.0494	0.0500	0.0249
Q_{C23}(p.u.)	0.0338	0.0449	0.0264	0.0421
Q_{C24}(p.u.)	0.0292	0.0434	0.0500	0.0424
Q_{C29}(p.u.)	0.0069	0.0491	0.0500	0.0457
F_{cost} (\$/h)	837.5766	**832.0140**	835.1034	832.3203
F_{loss} (MW)	5.0926	**5.0766**	5.0658	5.0796

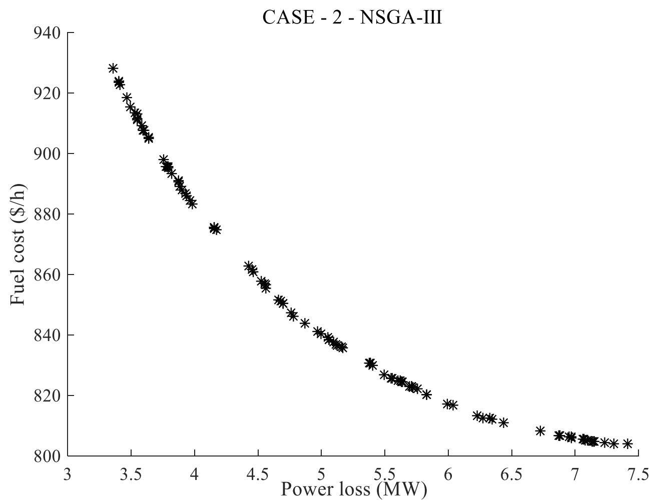

Fig. 10. PF of CASE-2 obtained by NSGA-III

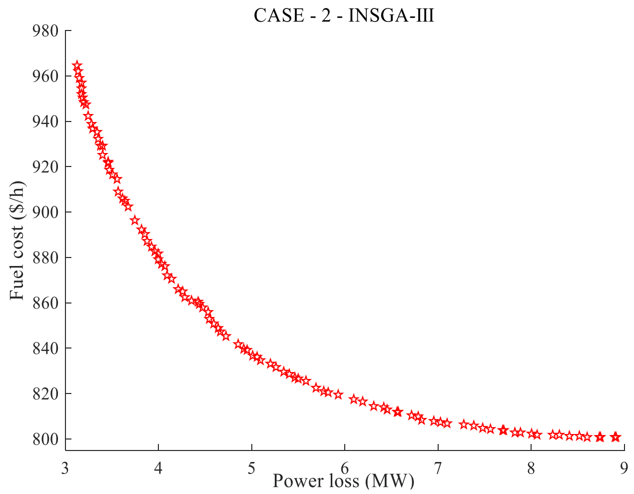

Fig. 11. PF of CASE-2 obtained by INSGA-III

TABLE XI
MINIMAL SOLUTIONS OF CASE-2

Variables	CASE-2			
	Minimal F_{cost}		Minimal F_{loss}	
	NSGA-III	INSGA-III	NSGA-III	INSGA-III
P_{G2}(MW)	51.1181	49.9739	60.2227	78.6055
P_{G5}(MW)	20.7737	22.2181	49.5555	50.0000
P_{G8}(MW)	32.8864	21.4304	34.2479	34.9974
P_{G11}(MW)	15.6043	11.6367	29.5579	29.9772
P_{G13}(MW)	15.2981	12.0003	39.2370	40.0000
V_{G1}(p.u.)	1.0967	1.0830	1.0703	1.0784
V_{G2}(p.u.)	1.0768	1.0668	1.0628	1.0706
V_{G5}(p.u.)	1.0504	1.0274	1.0440	1.0604
V_{G8}(p.u.)	1.0595	1.0401	1.0554	1.0642
V_{G11}(p.u.)	1.0816	1.0743	1.0997	1.0681
V_{G13}(p.u.)	1.0990	1.0991	1.0892	1.0581
T_{11}(p.u.)	0.9471	0.9725	0.9832	1.0520
T_{12}(p.u.)	1.0038	0.9698	0.9688	0.9588
T_{15}(p.u.)	0.9803	0.9581	0.9768	0.9824
T_{36}(p.u.)	0.9499	0.9894	0.9745	0.9949
Q_{C10}(p.u.)	0.0480	0.0250	0.0451	0.0346
Q_{C12}(p.u.)	0.0094	0.0078	0.0180	0.0280
Q_{C15}(p.u.)	0.0423	0.0403	0.0437	0.0415
Q_{C17}(p.u.)	0.0064	0.0085	0.0142	0.0099
Q_{C20}(p.u.)	0.0038	0.0479	0.0261	0.0240
Q_{C21}(p.u.)	0.0452	0.0455	0.0472	0.0274
Q_{C23}(p.u.)	0.0143	0.0212	0.0222	0.0369
Q_{C24}(p.u.)	0.0260	0.0394	0.0241	0.0242
Q_{C29}(p.u.)	0.0094	0.0449	0.0166	0.0263
F_{loss}(MW)	7.4131	8.9075	3.3536	**3.1271**
F_{cost} ($/h)	803.9893	**800.6080**	928.0639	964.6998

TABLE XII
GD AND HV OF CASE-2

Quantitative indicators		GD		HV	
		Average	Deviation	Average	Deviation
CASE-2	NSGA-III	0.0955	0.0216	617.3241	47.8720
	INSGA-III	0.0808	0.0177	886.6208	42.7006

Additionally, the schemes with minimum single-objective of CASE-2 are shown in TABLE XI. The INSGA-III algorithm put forward in this paper obtains 800.6080 $/h of minimal F_{cost} and 3.1271 MW of minimal F_{loss}. Both minimal F_{cost} and F_{loss} goals found by INSGA-III method are smaller than the ones found by NSGA-III, which verifies the competitive edge of INSGA-III in solving MOOPF problems.

Furthermore, Fig. 12 and TABLE XII show the evaluation results of PF-distribution and PF-diversity according to GD and HV criteria. In addition to verifying the advantages of INSGA-III algorithm in PF-uniformity and PF-diversity, the smaller GD-deviation and HV-deviation values also prove the better consistency of results from 30 MOOPF independent experiments.

Meanwhile, three related errors of five candidate BP fuel-cost models for CASE-2 are given in TABLE XIII. The $N_{BP(2)}$ network with relatively-minimal MAE, MAPE and RMSE errors is adopted to explore the preferable EPL solutions of CASE-2. Then, the fitting results and relative error corresponding to $N_{BP(2)}$ network are given in Fig. 13 and Fig. 14.

The detail of Sch_{elite} candidate elite solutions for CASE-2 are shown in TABLE XIV. It indicates that four EPL solutions are obtained by proposed $N_{BP(2)}$ fuel-cost forecasting network. And the control variables of EPL schemes are given in TABLE XV.

3) CASE-3

In CASE-3, F_{cost}, F_{loss} and F_{emis} goals are optimized at the same time. Obviously, the triple-goal MOOPF case is more difficult than the double-goal ones and it can further verify the performance of INSGA-III algorithm.

The PFs of CASE-3, which are respectively obtained by NSGA-III and INSGA-III algorithms, are shown in Fig. 15 and Fig. 16. Fig. 16 clearly states that the presented INSGA-III method is also able to find the satisfactory PF even in the triple-goal MOOPF case.

TABLE XIII
ERRORS OF CANDIDATE NETWORKS FOR CASE-2

Networks	MAE	MAPE	RMSE
$N_{BP(1)}$	0.0441	5.2512E-05	0.0930
$N_{BP(2)}$	**0.0241**	**2.8809E-05**	**0.0362**
$N_{BP(3)}$	0.0373	4.4448E-05	0.0737
$N_{BP(4)}$	0.0377	4.5000E-05	0.0538
$N_{BP(5)}$	0.0576	6.8646E-05	0.1046

TABLE XIV
Sch_{elite} CANDIDATE ELITE SOLUTIONS OF CASE-2

Candidate	*Solution$_1$*	***Solution$_2$***	***Solution$_3$***	***Solution$_4$***	*Solution$_5$*
$Fuel_{pre}$	831.5948	**831.5999**	**831.6043**	**831.6077**	831.6088
F_{cost}	831.9510	**831.9339**	**831.9426**	**831.9225**	831.9401
F_{loss}	5.0827	**5.0759**	**5.0755**	**5.0765**	5.0832
Dominance	-	√	√	√	-
Candidate	*Solution$_6$*	*Solution$_7$*	*Solution$_8$*	*Solution$_9$*	***Solution$_{10}$***
$Fuel_{pre}$	831.6094	831.6129	831.6142	831.6262	**831.6359**
F_{cost}	831.9504	831.9374	831.9460	831.9659	**831.9667**
F_{loss}	5.0789	5.0804	5.0783	5.0819	**5.0743**
Dominance	-	-	-	-	√

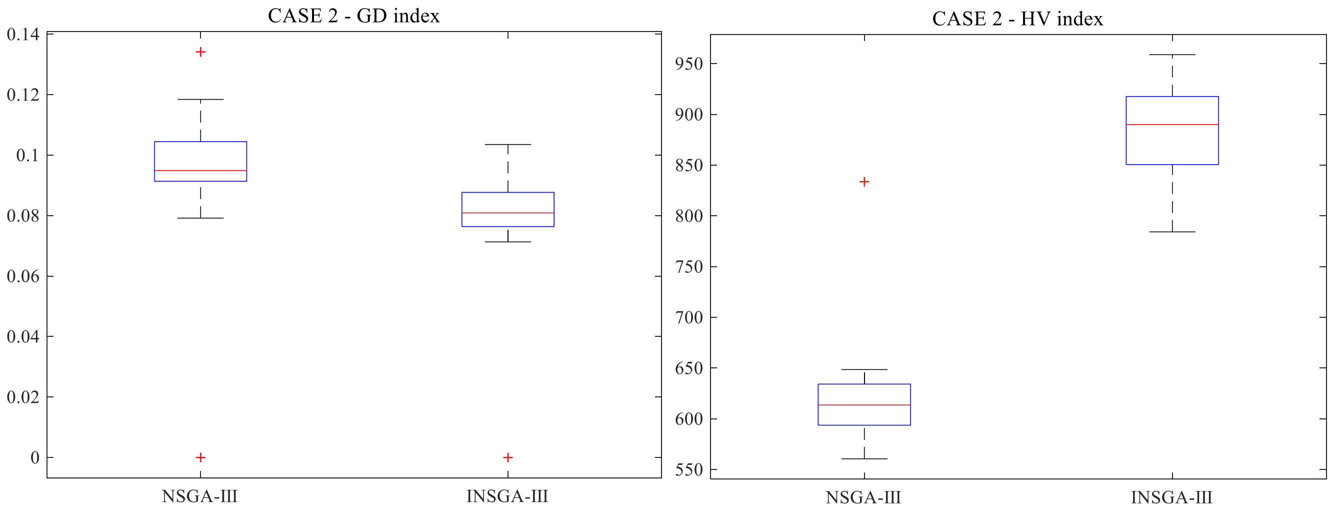

Fig. 12. Boxplot of GD and HV indexes for CASE-2

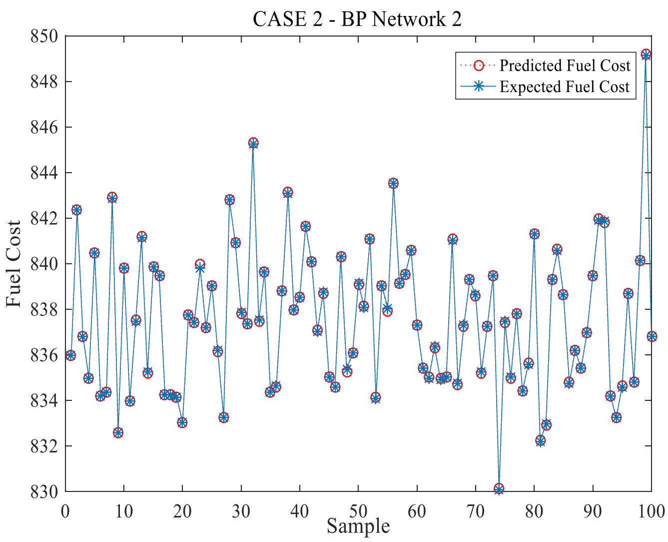

Fig. 13. Fitting results of CASE-2

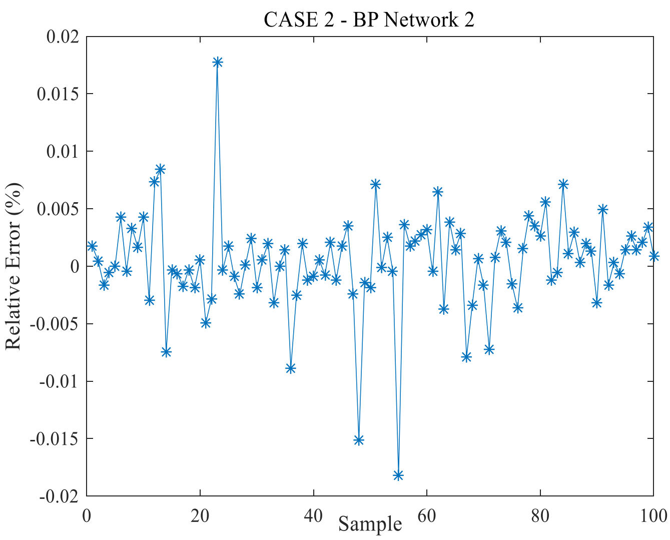

Fig. 14. Relative error of CASE-2

TABLE XV
EPL SOLUTIONS OF CASE-2

Variables	CASE-2			
	EPL_1	EPL_2	EPL_3	EPL_4
P_{G2}(MW)	52.2027	52.1697	52.1631	52.1698
P_{G5}(MW)	30.0363	30.0300	30.0395	30.0503
P_{G8}(MW)	35.0000	35.0000	35.0000	35.0000
P_{G11}(MW)	29.8691	29.8798	29.8797	29.8801
P_{G13}(MW)	22.2646	22.2869	22.2574	22.2779
V_{G1}(p.u.)	1.1000	1.1000	1.1000	1.1000
V_{G2}(p.u.)	1.0882	1.0881	1.0883	1.0884
V_{G5}(p.u.)	1.0645	1.0647	1.0638	1.0638
V_{G8}(p.u.)	1.0736	1.0734	1.0737	1.0733
V_{G11}(p.u.)	1.0993	1.1000	1.1000	1.1000
V_{G13}(p.u.)	1.1000	1.1000	1.0989	1.1000
T_{11}(p.u.)	1.0286	1.0284	1.0285	1.0285
T_{12}(p.u.)	0.9098	0.9098	0.9098	0.9098
T_{15}(p.u.)	0.9803	0.9803	0.9803	0.9802
T_{36}(p.u.)	0.9709	0.9709	0.9709	0.9710
Q_{C10}(p.u.)	0.0082	0.0082	0.0082	0.0082
Q_{C12}(p.u.)	0.0500	0.0500	0.0500	0.0500
Q_{C15}(p.u.)	0.0203	0.0203	0.0203	0.0203
Q_{C17}(p.u.)	0.0362	0.0362	0.0362	0.0362
Q_{C20}(p.u.)	0.0462	0.0462	0.0462	0.0462
Q_{C21}(p.u.)	0.0494	0.0494	0.0494	0.0494
Q_{C23}(p.u.)	0.0449	0.0449	0.0449	0.0449
Q_{C24}(p.u.)	0.0434	0.0434	0.0434	0.0434
Q_{C29}(p.u.)	0.0491	0.0491	0.0491	0.0491
F_{cost} ($/h)	831.9339	831.9426	831.9225	831.9667
F_{loss} (MW)	5.0759	5.0755	5.0765	5.0743

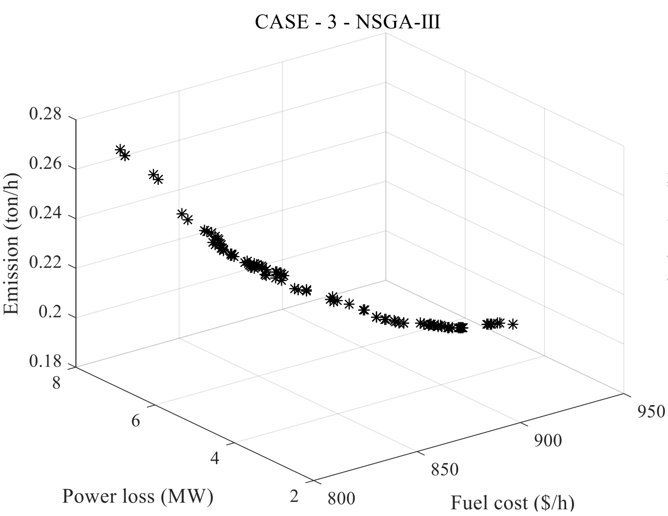

Fig. 15. PF of CASE-3 obtained by NSGA-III

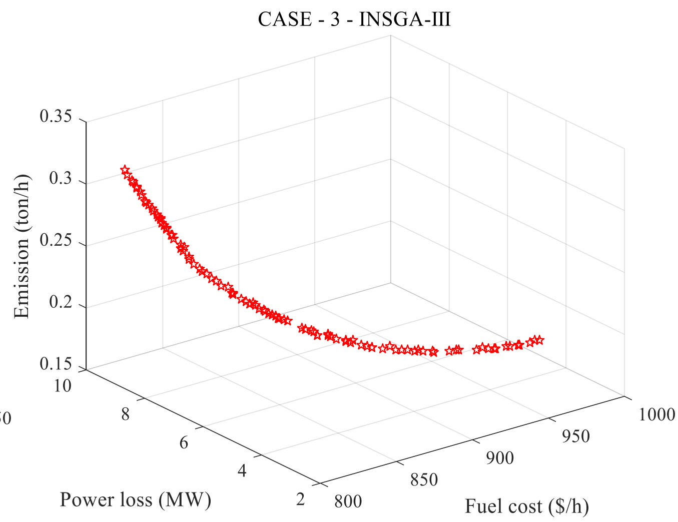

Fig. 16. PF of CASE-3 obtained by INSGA-III

TABLE XVI gives two BCS solutions and the comparison result found by the published MOFA-PFA method. The BCS of INSGA-III method composed by 876.9736 $/h of F_{cost}, 4.2439 MW of F_{loss} and 0.2073 ton/h of F_{emis} is superior to the relatively-best scheme of typical NSGA-III. Besides, TABLE XVII shows the minimal F_{cost} (799.5961 $/h), minimal F_{loss} (3.1242 MW), minimal F_{emis} (0.1943 ton/h) are all achieved by INSGA-III algorithm.

The errors of five fuel-cost prediction networks are shown in TABLE XVIII and the $N_{BP(3)}$ model with smaller MAE, MAPE, RMSE is finally adopted. For CASE-3, the fitting results and relative-error are, separately, given in Fig. 17 and Fig. 18.

Furthermore, TABLE XIX gives the detail of Sch_{elite} candidate elite solutions of CASE-3. It intuitively states that five EPL solutions of CASE-3 are determined. Although the prediction effect of the tri-objective MOOPF case is not as good as that of the bi-objective one, the brand-new $N_{BP(3)}$ model still finds multiple EPL solutions. The control variables of five EPL scheme are shown in TABLE XX.

TABLE XVI
BCS AND COMPARISON OF CASE-3

Variables	CASE-3 NSGA-III	CASE-3 INSGA-III	CASE-3 MOFA-PFA [30]
P_{G2}(MW)	65.1562	61.4422	57.890
P_{G5}(MW)	37.3055	37.1152	36.290
P_{G8}(MW)	29.8221	34.0397	35.000
P_{G11}(MW)	29.5921	29.7562	29.271
P_{G13}(MW)	35.4797	35.8105	40.000
V_{G1}(p.u.)	1.0343	1.0890	1.0985
V_{G2}(p.u.)	1.02146	1.0788	1.0869
V_{G5}(p.u.)	0.9952	1.0652	1.0625
V_{G8}(p.u.)	1.0013	1.0673	1.0767
V_{G11}(p.u.)	1.0231	1.0228	1.0857
V_{G13}(p.u.)	1.0392	1.0387	1.0386
T_{11}(p.u.)	1.0080	1.0535	1.0860
T_{12}(p.u.)	0.9768	0.9129	0.9930
T_{15}(p.u.)	1.0220	1.0199	1.0520
T_{36}(p.u.)	0.9688	0.9846	1.0770
Q_{C10}(p.u.)	0.0454	0.0428	0.0140
Q_{C12}(p.u.)	0.0325	0.0203	0.020
Q_{C15}(p.u.)	0.0050	0.0500	0.0080
Q_{C17}(p.u.)	0.0278	0.0409	0.0250
Q_{C20}(p.u.)	0.0223	0.0086	0.0390
Q_{C21}(p.u.)	0.0087	0.0271	0.0270
Q_{C23}(p.u.)	0.0294	0.0359	0.0100
Q_{C24}(p.u.)	0.0500	0.0191	0.0170
Q_{C29}(p.u.)	0.0130	0.0213	0.0500
F_{cost} (\$/h)	878.1387	**876.9736**	879.91
F_{loss} (MW)	4.7932	**4.2439**	4.2179
F_{emis} (ton/h)	0.2092	**0.2073**	0.2165

TABLE XVII
MINIMAL SOLUTIONS OF CASE-3

Variables	CASE-3					
	Minimal F_{cost}		Minimal F_{loss}		Minimal F_{emis}	
	NSGA-III	INSGA-III	NSGA-III	INSGA-III	NSGA-III	INSGA-III
P_{G2}(MW)	57.1339	48.4456	65.3614	79.3481	65.3614	72.7707
P_{G5}(MW)	23.4779	21.5648	49.0766	50.0000	49.0766	50.0000
P_{G8}(MW)	34.8481	22.2846	30.8966	35.0000	30.8966	35.0000
P_{G11}(MW)	18.7528	11.8287	30.0000	29.5703	30.0000	30.0000
P_{G13}(MW)	15.3990	12.0000	40.0000	40.0000	40.0000	40.0000
V_{G1}(p.u.)	1.0541	1.1000	1.0236	1.0873	1.0236	1.0870
V_{G2}(p.u.)	1.0389	1.0809	1.0154	1.0810	1.0154	1.0810
V_{G5}(p.u.)	0.9862	1.0608	0.9883	1.0673	0.9883	1.0648
V_{G8}(p.u.)	0.9986	1.0634	1.0090	1.0696	1.0090	1.0673
V_{G11}(p.u.)	1.0410	1.0545	1.0366	1.0474	1.0366	1.0487
V_{G13}(p.u.)	1.0173	1.0809	1.0485	1.0365	1.0485	1.0320
T_{11}(p.u.)	0.9683	1.0896	0.9930	1.0734	0.9930	1.0715
T_{12}(p.u.)	1.0375	0.9394	0.9926	0.9204	0.9926	0.9194
T_{15}(p.u.)	0.9646	1.0151	0.9512	0.9989	0.9512	0.9859
T_{36}(p.u.)	0.9551	1.0006	0.9214	1.0168	0.9214	1.0126
Q_{C10}(p.u.)	0.0435	0.0496	0.0403	0.0412	0.0403	0.0420
Q_{C12}(p.u.)	0.0305	0.0231	0.0301	0.0196	0.0301	0.0198
Q_{C15}(p.u.)	0.0200	0.0324	0.0050	0.0463	0.0050	0.0462
Q_{C17}(p.u.)	0.0419	0.0412	0.0325	0.0414	0.0325	0.0411
Q_{C20}(p.u.)	0.0142	0.0080	0.0178	0.0110	0.0178	0.0111
Q_{C21}(p.u.)	0.0240	0.0390	0.0174	0.0287	0.0174	0.0296
Q_{C23}(p.u.)	0.0442	0.0375	0.0393	0.0361	0.0393	0.0361
Q_{C24}(p.u.)	0.0406	0.0285	0.0500	0.0179	0.0500	0.0186
Q_{C29}(p.u.)	0.0125	0.0124	0.0077	0.0206	0.0077	0.0220
F_{cost} (\$/h)	813.1989	**799.5961**	932.9870	965.4179	932.9870	953.3341
F_{loss} (MW)	7.5542	8.6646	3.9027	**3.1242**	3.9027	3.1834
F_{emis} (ton/h)	0.2681	0.3268	0.1974	0.1950	0.1974	**0.1943**

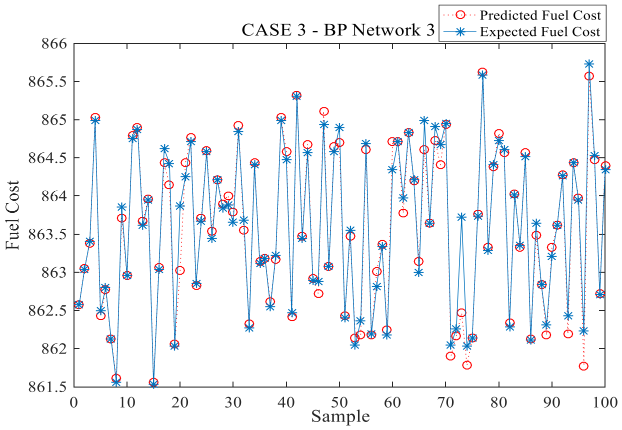

Fig. 17. Fitting results of CASE-3

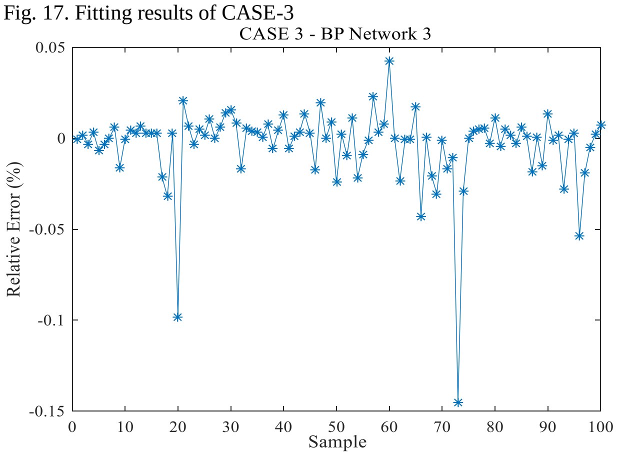

Fig. 18. Relative error of CASE-3

TABLE XVIII
ERRORS OF CANDIDATE NETWORKS FOR CASE-3

Networks	MAE	MAPE	RMSE
$N_{BP(1)}$	0.1437	1.6644E-4	0.2688
$N_{BP(2)}$	0.1905	2.2066 E-4	0.2754
$\boldsymbol{N_{BP(3)}}$	**0.0999**	**1.1562 E-4**	**0.1927**
$N_{BP(4)}$	0.1872	2.1683 E-4	0.4364
$N_{BP(5)}$	0.1943	2.2498E-4	0.3287

TABLE XIX
Sch_{elite} CANDIDATE ELITE SOLUTIONS OF CASE-3

Candidate	*Solution*$_1$	***Solution*$_2$**	*Solution*$_3$	***Solution*$_4$**	*Solution*$_5$
$Fuel_{pre}$	877.8448	**877.8496**	877.8514	**877.8550**	877.8553
F_{cost}	876.9547	**876.9620**	876.9619	**876.9630**	876.9643
F_{loss}	4.2442	**4.2437**	4.2452	**4.2439**	4.2445
F_{emis}	0.2073	**0.2073**	0.2073	**0.2073**	0.2073
Dominance	-	√	-	√	-
Candidate	***Solution*$_6$**	*Solution*$_7$	***Solution*$_8$**	*Solution*$_9$	***Solution*$_{10}$**
$Fuel_{pre}$	**877.8589**	877.8590	**877.8591**	877.8602	**877.8602**
F_{cost}	**876.9680**	876.9685	**876.9652**	876.9714	**876.9658**
F_{loss}	**4.2435**	4.2440	**4.2438**	4.2448	**4.2427**
F_{emis}	**0.2073**	0.2073	**0.2073**	0.2073	**0.2073**
Dominance	√	-	√	-	√

TABLE XX
EPL SOLUTIONS OF CASE-3

Variables	CASE-3				
	EPL_1	EPL_2	EPL_3	EPL_4	EPL_5
P_{G2}(MW)	61.4413	61.4453	61.4445	61.4367	61.4419
P_{G5}(MW)	37.1136	37.1127	37.1155	37.1148	37.1118
P_{G8}(MW)	34.0383	34.0420	34.0366	34.0430	34.0411
P_{G11}(MW)	29.7559	29.7542	29.7550	29.7545	29.7587
P_{G13}(MW)	35.8090	35.8075	35.8093	35.8100	35.8103
V_{G1}(p.u.)	1.0890	1.0890	1.0891	1.0890	1.0890
V_{G2}(p.u.)	1.0789	1.0788	1.0788	1.0787	1.0789
V_{G5}(p.u.)	1.0652	1.0652	1.0651	1.0651	1.0651
V_{G8}(p.u.)	1.0672	1.0674	1.0673	1.0674	1.0674
V_{G11}(p.u.)	1.0228	1.0229	1.0228	1.0229	1.0228
V_{G13}(p.u.)	1.0387	1.0386	1.0388	1.0387	1.0388
T_{11}(p.u.)	1.0535	1.0535	1.0535	1.0535	1.0535
T_{12}(p.u.)	0.9129	0.9129	0.9129	0.9129	0.9129
T_{15}(p.u.)	1.0199	1.0199	1.0199	1.0199	1.0199
T_{36}(p.u.)	0.9846	0.9846	0.9846	0.9846	0.9846
Q_{C10}(p.u.)	0.0428	0.0428	0.0428	0.0428	0.0428
Q_{C12}(p.u.)	0.0203	0.0203	0.0203	0.0203	0.0203
Q_{C15}(p.u.)	0.0500	0.0500	0.0500	0.0500	0.0500
Q_{C17}(p.u.)	0.0409	0.0409	0.0409	0.0409	0.0409
Q_{C20}(p.u.)	0.0086	0.0086	0.0086	0.0086	0.0086
Q_{C21}(p.u.)	0.0271	0.0271	0.0271	0.0271	0.0271
Q_{C23}(p.u.)	0.0359	0.0359	0.0359	0.0359	0.0359
Q_{C24}(p.u.)	0.0191	0.0191	0.0191	0.0191	0.0191
Q_{C29}(p.u.)	0.0213	0.0213	0.0213	0.0213	0.0213
F_{cost} ($/h)	876.9620	876.9630	876.9680	876.9652	876.9658
F_{loss} (MW)	4.2437	4.2439	4.2435	4.2438	4.2427
F_{emis} (ton/h)	0.2073	0.2073	0.2073	0.2073	0.2073

It is very difficult to find the EPL solutions with all three goals smaller than the current BCS. Thrillingly, the presented BP fuel-cost model can effectively solve the mentioned difficulties.

V. Conclusion

To explore the high-performance scheduling schemes with zero constraints-violation, the modified INSGA-III algorithm and an innovative fuel-cost forecasting network are proposed. Combining with NAD dominant strategy, the presented INSGA-III algorithm achieves the evenly-distributed PFs. Furthermore, the novel BP fuel-cost prediction model is put forward and it successfully finds more than four EPL solutions near the current BCS solution. Numerous results strongly prove the applicability and advantages of proposed INSGA-III algorithm and BP fuel-cost model in both double-goal and triple-goal MOOPF problems.

In conclusion, the advanced computer technologies such as neural networks and intelligence algorithms offer another powerful way to handle the complex MOOPF problems.

References

[1] G. Chen, J. Qian, Z. Zhang and S. Li, "Application of modified pigeon-inspired optimization algorithm and constraint-objective sorting rule on multi-objective optimal power flow problem", *Applied Soft Computing*, vol. 92, pp106321, 2020.

[2] G. Guo, J. Qian and S. Li, "Optimal power flow based on novel multi-objective artificial fish swarm algorithm", *Engineering Letters*, vol. 2, no. 28, pp542-550, 2020.

[3] S. Khunkitti, A. Siritaratiwat, S. Premrudeepreechacharn, R. Chatthaworn and N. Watson, "A hybrid DA-PSO optimization algorithm for multiobjective optimal power flow problems", *Energies*, vol. 11, no. 9, pp2270, 2018.

[4] W. W, H. Hashim, M. Norman, W. Noor and I. Abdul, "A novel quasi-oppositional modified Jaya algorithm for multi-objective optimal power flow solution", *Applied Soft Computing*, vol. 65, pp360-373, 2018.

[5] G. Chen, X. Yi, Z. Zhang and H. Wang, "Applications of multi-objective dimension-based firefly algorithm to optimize the power losses, emission, and cost in power systems", *Applied Soft Computing*, vol. 68, pp322-342, 2018.

[6] X. Yuan, et al., "Multi-objective optimal power flow based on improved strength Pareto evolutionary algorithm", *Energy*, vol. 122, pp70-82, 2017.

[7] G. Chen, S. Qiu, Z. Zhang and Z. Sun, "Quasi-oppositional cuckoo search algorithm for multi-objective optimal power flow", *IAENG International Journal of Computer Science*, vol. 45, no. 2, pp255-266, 2018.

[8] G. Chen, J. Qian, Z. Zhang and Z. Sun, "Applications of novel hybrid bat algorithm with constrained Pareto fuzzy dominant rule on multi-objective optimal power flow problems", *IEEE Access*, vol. 7, pp52060-52084, 2019.

[9] X. Yuan, P. Wang, Y. Yuan, Y. Huang and X. Zhang, "A new quantum inspired chaotic artificial bee colony algorithm for optimal power flow problem", *Energy Conversion and Management*, vol. 100, pp1-9, 2015.

[10] J.B. Hmida, M.J. Morshed, J. Lee and T. Chambers, "Hybrid imperialist competitive and grey wolf algorithm to solve multiobjective optimal power flow with wind and solar units", *Energies*, vol. 11, no. 11, pp2891, 2018.

[11] M. Ghasemi, S. Ghavidel, M.M. Ghanbarian, M. Gharibzadeh and A. Azizi Vahed, "Multi-objective optimal power flow considering the cost, emission, voltage deviation and power losses using multi-objective modified imperialist competitive algorithm", *Energy*, vol. 78, pp276-289, 2014.

[12] S. Rahmani and N. Amjady, "Improved normalised normal constraint method to solve multi-objective optimal power flow problem", *IET Generation Transmission and Distribution*, vol. 12, no. 4, pp859-872, 2018.

[13] G. Chen, L. Zhengmei and Z. Zhizhong, "Improved krill herd algorithm with novel constraint handling method for solving optimal power flow problems", *Energies*, vol. 11, no. 1, pp76, 2018.

[14] G. Chen, J. Qian, Z. Zhang and Z. Sun, "Many-objective new bat algorithm and constraint-priority non-inferior sorting strategy for optimal power flow", *Engineering Letters*, vol. 27, no. 4, pp882-892, 2019.

[15] M. Ding, H. Chen, N. Lin, et al., "Dynamic population artificial bee colony algorithm for multi-objective optimal power flow", *Saudi Journal of Biological Sciences*, vol. 24, no. 3, pp703-710, 2017.

[16] A.F. Attia, R.A.El Sehiemy and H.M. Hasanien, "Optimal power flow solution in power systems using a novel Sine-Cosine algorithm", *International Journal of Electrical Power and Energy Systems*, vol. 99, pp331-343, 2018.

[17] H. PulluriR. Naresh and V. Sharma, "An enhanced self-adaptive differential evolution based solution methodology for multiobjective optimal power flow", *Applied Soft Computing*, vol. 54, pp229-245, 2017.

[18] G. Guo, J. Qian and S. Li, " Novel many-objective NSGA-FA algorithm to minimize fuel cost, power loss and emission of electric systems", *IAENG International Journal of Computer Science*, vol. 47, no. 4, pp634-644, 2020.

[19] G. Chen, J. Qian, Z. Zhang and Z. Sun, "Multi-objective improved bat algorithm for optimizing fuel cost, emission and active power loss in power system", *IAENG International Journal of Computer Science*, vol. 46, no. 1, pp118-133, 2019.

[20] K. Deb, A. Pratap, S. Agarwal and T. Meyarivan, "A fast and elitist multiobjective genetic algorithm: NSGA-II", *IEEE Transactions on Evolutionary Computatio*n, vol. 2, no. 6, pp182-197, 2002.

[21] H. Li, K. Deb, Q. Zhang, P.N. Suganthan and L. Chen, "Comparison between MOEA/D and NSGA-III on a set of many and multi-objective benchmark problems with challenging difficulties", *Swarm and Evolutionary Computation*, vol. 46, pp104-117, 2019.

[22] P.C. RoyK. Deb and M.M. Islam, "An Efficient nondominated sorting algorithm for large number of fronts", *IEEE Transactions on Cybernetics*, vol. 49, no. 3, pp859-869, 2019.

[23] J. Zhang, S. Wang, Q. Tang, Y. Zhou and T. Zeng, "An improved NSGA-III integrating adaptive elimination strategy to solution of many-objective optimal power flow problems", *Energy*, vol. 172, pp945-957, 2019.

[24] Y. WuR. Gao and J. Yang, "Prediction of coal and gas outburst: a method based on the BP neural network optimized by GASA", *Process Safety and Environmental Protection*, vol. 133, pp64-72, 2020.

[25] Z. Pu and X. Wang, "Finite-time convergent complex-valued neural networks for computing square root of complex matrices", *IAENG International Journal of Applied Mathematics*, vol. 50, no. 3, pp512-518, 2020.

[26] G. Chen, J. Chen, Z. Zhang and Z. Sun, "Short-Term Wind Speed Forecasting Based on Fuzzy C-Means Clustering and Improved MEA-BP", *IAENG International Journal of Computer Science*, vol. 46, no. 4, pp768-776, 2019.

[27] G. Xiong and D. Shi, "Orthogonal learning competitive swarm optimizer for economic dispatch problems", *Applied Soft Computing*, vol. 66, pp134-148, 2018.

[28] D. Narges, T. Saeed, H. Mehrdad and Tarafdar, "Adaptive group search optimization algorithm for multi-objective optimal power flow problem", *Applied Soft Computing*, vol. 38, pp1012-1024, 2016.

[29] G. Chen, J. Qian, Z. Zhang and Z. Sun, "Multi-objective optimal power flow based on hybrid firefly-bat algorithm and constraints-prior object-fuzzy sorting strategy", *IEEE Access*, vol. 7, pp139726-139745, 2019.

[30] G. Chen, X. Yi, Z. Zhang and H. Lei, "Solving the multi-objective optimal power flow problem using the multi-objective firefly algorithm with a constraints-prior Pareto-domination approach", *Energies*, vol. 11, no. 12, pp3438, 2018.